

Turbulence in Magnetic Reconnection Jets from Injection to Sub-Ion Scales

Louis Richard¹^{*}

*Swedish Institute of Space Physics, Uppsala 751 21, Sweden
and Department of Physics and Astronomy, Space and Plasma Physics, Uppsala University, Uppsala 751 20, Sweden*

Luca Sorriso-Valvo²

*CNR/ISTP—Istituto per la Scienza e la Tecnologia dei Plasmi, 70126 Bari, Italy;
Space and Plasma Physics, School of Electrical Engineering and Computer Science,
KTH Royal Institute of Technology, Stockholm 114 28, Sweden;
and Swedish Institute of Space Physics, Uppsala 751 21, Sweden*

Emiliya Yordanova³, Daniel B. Graham³, and Yuri V. Khotyaintsev³

Swedish Institute of Space Physics, Uppsala 751 21, Sweden



(Received 16 March 2023; revised 2 October 2023; accepted 5 February 2024; published 4 March 2024)

We investigate turbulence in magnetic reconnection jets in the Earth's magnetotail using data from the Magnetospheric Multiscale spacecraft. We show that signatures of a limited inertial range are observed in many reconnection jets. The observed turbulence develops on the timescale of a few ion gyroperiods, resulting in intermittent multifractal energy cascade from the characteristic scale of the jet down to the ion scales. We show that at sub-ion scales, the fluctuations are close to monofractal and predominantly kinetic Alfvén waves. The observed energy transfer rate across the inertial range is $\sim 10^8 \text{ J kg}^{-1} \text{ s}^{-1}$, which is the largest reported for space plasmas so far.

DOI: 10.1103/PhysRevLett.132.105201

The interplay between the two ubiquitous phenomena, magnetic reconnection and turbulence, is a long-standing problem in collisionless plasmas [1]. Magnetic reconnection is a process that provides energization and acceleration of plasma through explosive topological reconfiguration of the magnetic field [2,3]. It is responsible for the generation of fast plasma flows (jets) as observed, for example, in solar flares [4], black hole flares [5] and planetary magnetotails [3]. In the reconnection region, turbulence and wave growth due to kinetic processes can, in turn, affect the dynamics of the magnetic reconnection [6]. On the other hand, turbulence is a universal process that transfers kinetic and magnetic energy from large injection scales to small scales through an energy cascade produced by nonlinear interactions among fluctuations [7,8]. If the turbulence is fully developed, such energy transfer is globally scale invariant over a range of scales, called the inertial range, where large-scale forcing and small-scale dissipation can be neglected. This produces power-law scaling of statistical quantities, such as the power spectral density and the moments of the scale-dependent fluctuations [8].

In addition, spatial inhomogeneity of the energy transfer results in intermittency, i.e., formation of spatially concentrated structures such as current sheets and vortices [9] where dissipation occurs [10].

Numerical simulations show that turbulence develops in reconnection jets, resulting in the formation of secondary reconnection sites [11] and intermittent magnetic field fluctuations at kinetic scales (smaller than the ion gyroscale) [12,13]. *In situ* spacecraft observations in reconnection jets suggest development of turbulence [14–17], forming current sheets where energy is dissipated [16,18]. The interaction of the particles with the turbulence-generated secondary magnetic flux ropes and other spatially concentrated structures provides efficient particle heating and acceleration through the Fermi mechanism [19–25]. Therefore, a complete description of the turbulent energy transfer from injection to sub-ion scales is crucial to understand the energization of the content of collisionless plasma jets. However, the transient nature of reconnection jets yields short samples of *in situ* measurements, and thus, it is difficult to obtain a meaningful statistical description of the fluctuations [26]. As a result, the complex interplay between magnetic reconnection and turbulence in reconnection jets remains unclear.

In this Letter, we use data from the Magnetospheric Multiscale (MMS) spacecraft [27] in the terrestrial

Published by the American Physical Society under the terms of the Creative Commons Attribution 4.0 International license. Further distribution of this work must maintain attribution to the author(s) and the published article's title, journal citation, and DOI. Funded by Bibsam.

magnetosphere to investigate turbulence in reconnection jets. We study 330 plasma jets in the plasma sheet of the Earth's magnetotail ($\beta_i \geq 0.5$, where $\beta_i = 2\mu_0 n_i k_B T_i / B^2$, n_i is the ion number density, T_i the ion temperature, and B the magnetic field magnitude); see Ref. [28] for a detailed description of the data. The jets are observed in the midtail, $-15R_E \geq X_{GSM} \geq -25R_E$ in geocentric solar magnetospheric (GSM) coordinates; $R_E \approx 6371$ km is the Earth's radius. Magnetic reconnection is the primary driver of fast plasma flows in this part of the magnetotail [29,30]. The statistical location of the reconnection X-line for our dataset is $X_{GSM} \approx -25R_E$ [28]. Other mechanisms to generate jets (e.g., kinetic ballooning or interchange [31,32]) would be effective only in the near-Earth tail, $X_{GSM} \geq -15R_E$, which is outside of the region we study. Therefore, we assume that the observed jets are generated by reconnection. We use magnetic field measurements from MMS's FGM instrument [33] and electric field measurements from the EDP instrument [34,35]. The moments of the ion and electron velocity distributions are measured by the FPI instrument [36] with corrections removing low-energy photoelectrons and a background ion population to account for penetrating radiation [37].

Figure 1 presents an example of a fast ($|V_i| \geq 300$ km s $^{-1}$ with V_i the ion bulk velocity) Earthward jet [Fig. 1(c)]. We see enhanced fluctuations in the magnetic field \mathbf{B} and electric field \mathbf{E} [Figs. 1(a) and 1(b)]. The correlation scale, i.e., the size of the energy-containing eddies [38,39], is $l_c = 53d_i = 3.7R_E$, where $d_i = \sqrt{m_i/n_i e^2 \mu_0}$ is the ion inertial length (see Supplemental Material [40]). Here, we use temporal-to-spatial scale equivalence $l_\perp = V\tau$, with $V = \langle |V_i| \rangle$, after verifying the validity of the Taylor hypothesis of frozen-in-flow fluctuations [41,42] and the assumption of anisotropic fluctuations (see Supplemental Material [40]). The power spectra of the electromagnetic fluctuations [Fig. 1(d)] exhibit a Kolmogorov-like power-law scaling, $|\mathbf{k}_\perp|^{-5/3}$ [71] in a range spanning from the energy injection scale, estimated as the correlation scale l_c , down to the ion gyroscale $\rho_i = \sqrt{\beta_i} d_i \approx 619$ km. At sub-ion scales, the magnetic field spectrum steepens to $|\mathbf{k}_\perp|^{-2.8}$ while the electric field spectrum rises to $|\mathbf{k}_\perp|^{-0.8}$, due to the contribution of the Hall term in the generalized Ohm's law at the ion kinetic scales [72,73]. The observed Kolmogorov spectrum at large scales ($l_c \geq l_\perp \geq \rho_i$) suggests global scale-invariant energy transfer across these scales.

In fully developed turbulence, the power spectrum (equivalent to the second-order moment of the fluctuations) is not sufficient to describe the fluctuations due to the intermittency [74]. Hence, we compute the structure functions of the magnetic field $S_m(\tau) = \langle |\Delta\mathbf{B}(\tau)|^m \rangle = \langle |\mathbf{B}(t + \tau) - \mathbf{B}(t)|^m \rangle$ with τ the timescale and $\langle \cdot \rangle$ the ensemble time average, having verified ergodicity and statistical convergence (see Supplemental Material [40]). We observe a power-law scaling $S_m(\tau) \propto \tau^{\zeta(m)}$ at large scales [Fig. 1(e)], which confirms the global scale-invariant

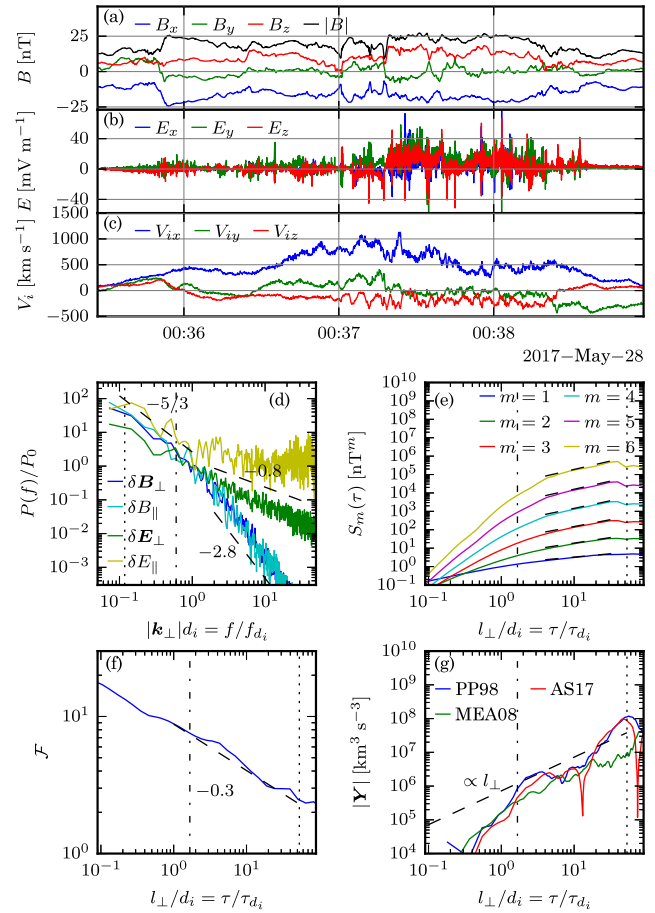


FIG. 1. Example of a reconnection jet with signatures of fully developed turbulence. (a) Magnetic field, (b) electric field, and (c) ion bulk velocity in GSM coordinates; (d) power spectral density of the electromagnetic fields normalized to $P_0 = P(f_{d_i})$, where $f_{d_i} = V/2\pi d_i$; (e) structure functions and (f) flatness of the magnetic field; (g) energy flux $|\mathbf{Y}|$. The dotted lines in panels (d)–(g) indicate the correlation scale l_c . The dashed-dotted lines in panels (d) and (e)–(g) indicate $|\mathbf{k}_\perp| \rho_i = 1$ and $l_\perp = \rho_i$, respectively. The dashed lines in panels (d)–(g) are reference power laws.

nature of the fluctuations. In addition, the flatness $\mathcal{F}(\tau) = S_4(\tau)/S_2^2(\tau)$, which measures the wings of the distribution of $\Delta\mathbf{B}(\tau)$, i.e., the occurrence of large gradients, is monotonically increasing as the scale decreases [Fig. 1(f)] indicating intermittency [8]. This provides evidence for spatially inhomogeneous energy transfer at large scales.

Knowledge of the energy transfer rate by the turbulence cascade across the scales is crucial to understanding the energy budget in the reconnection jets. We estimate the energy cascade rate using the third-order law for three-dimensional single-fluid magnetohydrodynamic (MHD) turbulence under the assumption of scale separation between injection and dissipation, homogeneity, and time stationarity of the fluctuations [43–45],

$$-2\epsilon = \frac{1}{2} \nabla_l \cdot Y + S, \quad (1)$$

where ϵ is the energy cascade rate, Y is the energy flux, and S is the energy source term, which is commonly assumed to be negligible compared with the flux terms [46]. Using various assumptions, Eq. (1) can be simplified to formulations which can be applied to spacecraft measurements. We employ the anisotropic incompressible (MEA08) [44], the isotropic incompressible (PP98) [43] and the isotropic compressible (AS17) [45] formulations, described in detail in the Supplemental Material [40]. The results from the three formulations are consistent within 1.3 standard deviations [Fig. 1(g)]. This is a good agreement given the uncertainties; therefore, the three formulations provide a reasonable order of magnitude estimate of $|Y|$. The energy flux $|Y|$ shows a scaling in l_\perp close to linear over a decade $\rho_i \leq l_\perp \leq l_c$, corresponding to an approximately constant energy cascade rate ϵ ; this behavior is qualitatively similar to previous *in situ* observations and numerical simulations [75]. This suggests that the third-order law is approximately satisfied across a limited scale range of one order of magnitude. We use the average between the three formulations $\epsilon = (|\epsilon_{\text{PP98}}| + |\epsilon_{\text{MEA08}}| + |\epsilon_{\text{AS17}}|)/3$ as an order of magnitude measure of the energy cascade rate. It yields, $\epsilon \approx 8.4 \pm 4.2 \times 10^8 \text{ J kg}^{-1} \text{ s}^{-1}$, which is the largest energy transfer rate ever calculated from *in situ* data [47,76–78].

Our analysis of the statistical properties of turbulence in this example reconnection jet indicates that the energy is transferred in a spatially inhomogeneous manner across a limited inertial range. To our knowledge, this is the first observation of third-order laws in magnetized ($\beta_i \approx 2.6$) reconnection jets.

To provide a complete systematic description of turbulence in magnetotail reconnection jets, we form an ensemble of 24 cases that show signatures of fully developed turbulence in the statistical sense introduced in the example. In the other 306 out of 330 cases, it is unclear if turbulence is developing, absent, suppressed, or statistical convergence is not achieved. We analyze the properties of the ensemble average of the 24 reconnection jets [Fig. 2] after normalizing the spatial scales to the ion inertial length d_i to account for the variability of the plasma conditions. This procedure results in a robust reference sample of turbulence in reconnection jets [Fig. 2]. The ensemble-averaged magnetic field δB , electric field δE , and electron number density δn_e power spectra [Fig. 2(a)] show a clear power-law scaling from the injection scale l_c to the ion scales, with a spectral exponent -1.72 ± 0.03 , close to the Kolmogorov value. The injection scale is $l_c \sim 10\rho_{i0}$ [Fig. 3(a)] where ρ_{i0} is the ion gyroradius in the background field $B_0 = B_{\text{ext}}/2$ [79] with $B_{\text{ext}} = \sqrt{1+\beta_i}|\mathbf{B}|$ obtained from the pressure balance assumption [80]. This gives $l_c \approx 3R_E$, comparable to the typical dimension of the reconnection jet across the flow [81,82]. This

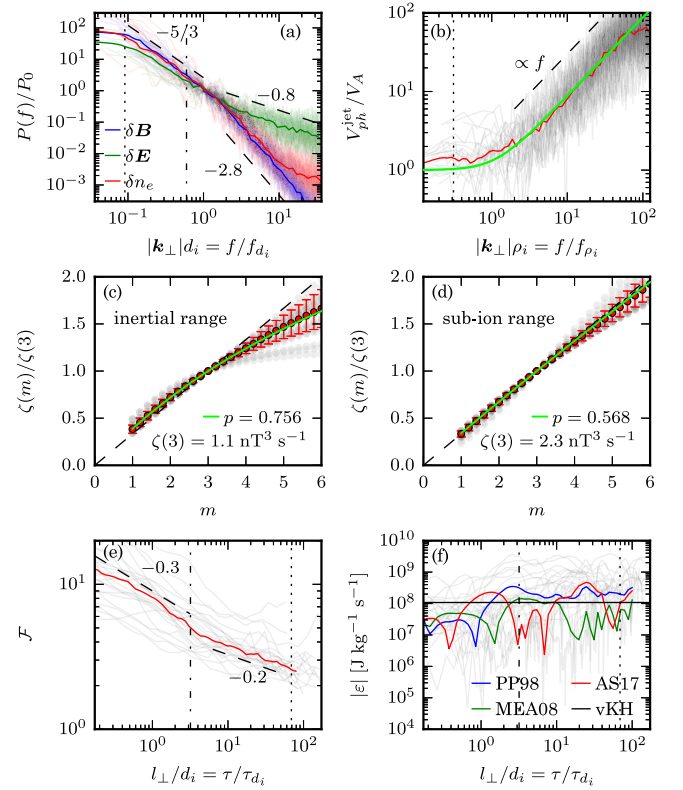


FIG. 2. Superposed analysis of the 24 reconnection jets. (a) Magnetic field, electric field, and electron number density power spectra; (b) normalized phase speed in the plasma frame; (c) and (d) scaling exponents of the structure functions in the inertial and sub-ion ranges, respectively; (e) flatness; (f) energy cascade rate. The thin transparent lines show the individual rescaled cases, and the solid lines show the ensemble averages. The green lines in panels (c) and (d) are fitted p model. The green line in panel (b) is the prediction for KAWs from Ref. [48]. The dotted lines in panels (a),(b),(e), and (f) indicate the average correlation scale l_c . The dashed-dotted lines in panels (a) and (e)–(f) indicate the average $|k_\perp|\rho_i = 1$ and $l_\perp = \rho_i$, respectively.

suggests that turbulence in the jet is generated by its relative motion with respect to the ambient plasma.

We now examine the energy balance in the 24 intervals. Assuming that the energy injection rate in the system corresponds to the decay rate of the energy-containing eddies [38], the former can be estimated using the von Kármán-Howarth energy decay law [43,83] $\epsilon_{\text{vKH}}^\pm = -d|\mathbf{Z}^\pm|^2/dt = C_{\text{vK}}^\pm |\mathbf{Z}^\pm|^2 |\mathbf{Z}^\mp|/l_c^\pm$, with l_c^\pm the correlation length of the Elsasser variables \mathbf{Z}^\pm and $C_{\text{vK}}^\pm \approx 0.03$ the von-Kármán constants [84]. On the other hand, using the ensemble signed average of ϵ from Eq. (1), we estimate the energy cascade rate $\langle \epsilon \rangle = (\langle \epsilon_{\text{PP98}} \rangle + \langle \epsilon_{\text{MEA08}} \rangle + \langle \epsilon_{\text{AS17}} \rangle)/3 \approx 1.8^{+1.1}_{-0.7} \times 10^8 \text{ J kg}^{-1} \text{ s}^{-1}$, positive and nearly constant at large scales, $l_c \geq l_\perp \geq \rho_i$ [Fig. 2(f)]. The obtained value is consistent with the ensemble average total von Kármán-Howarth energy decay rate $\langle \epsilon_{\text{vKH}} \rangle = (\langle \epsilon_{\text{vKH}}^+ \rangle + \langle \epsilon_{\text{vKH}}^- \rangle)/2 = 1.1^{+1.9}_{-0.3} \times 10^8 \text{ J kg}^{-1} \text{ s}^{-1}$. This indicates that the energy injected by magnetic reconnection in

the form of plasma jets is balanced by the turbulent energy transfer from the injection scale l_c to the ion scales. As a result, as seen in the power spectra [Fig. 2(a)], there is no energy accumulation across these scales.

To evaluate the contribution of the turbulent energy transfer to the magnetic reconnection process, we compare the energy cascade rate $\langle \varepsilon \rangle$ with the rate of decrease of magnetic energy in the reconnection inflow $\dot{\mathcal{E}}_b = (B_r^2/2\mu_0)/\Delta t$, where B_r is the reconnecting magnetic field and Δt is the duration. We note that in the approximation of Sweet-Parker reconnection, half of the energy inflow $\dot{\mathcal{E}}_b$ is available as kinetic energy in the outflow and the other half is dissipated to heating [85]. Assuming that $\Delta t \sim 100$ s is the typical duration of the transient reconnection [86] and $B_r = B_0 \sim 10$ nT, we obtain $\langle \varepsilon \rangle/\dot{\mathcal{E}}_b \sim 10\%$, suggesting that the turbulence transfers a substantial fraction of the magnetic reconnection energy input.

To understand how the energy is spatially distributed across the cascade, we analyze the high-order moments of the magnetic field fluctuations. The flatness [Fig. 2(e)] monotonically increases as the scale decreases from l_c to ρ_i , indicating a spatially inhomogeneous energy cascade at large scales. Using the structure functions $S_m(\tau)$ up to order $m = 6$, we find that the scaling exponents $\zeta(m)/\zeta(3)$ [Fig. 2(c)] show a nonlinear monotonic increase, providing evidence of a multifractal distribution of the energy conversion sites, i.e., intermittency [8]. Here, we normalize the scaling exponents to $\zeta(3) = 1.1 \pm 0.3$ to account for deviations from Kolmogorov's prediction $\zeta(3) = 1$ [87]. To quantitatively estimate the spatial inhomogeneity of the energy cascade, we fit the observed $\zeta(m)$, with $1 \leq m \leq 4$, to the multifractal p model $\zeta(m)/\zeta(3) = 1 - \log_2[p^{m(\alpha-1)/2} + (1-p)^{m(\alpha-1)/2}]$ [49], where $p \in [0.5, 1]$ is the intermittency parameter ($p = 0.5$ for monofractal non-intermittent fluctuations and $p = 1$ for maximum intermittency) and $\alpha = \zeta(2)/\zeta(3) + 1 = 1.72 \pm 0.03$ the spectral exponent [Fig. 2(a)]. We find that the normalized scaling exponents $\zeta(m)/\zeta(3)$ [Fig. 2(c)] are well described by the p -model with $p = 0.756 \pm 0.001$. This confirms that in the reconnection jets, the energy cascades at large scales in a multifractal, spatially inhomogeneous manner.

The statistical results described above provide evidence that an energy cascade is ongoing in this ensemble of reconnection jets at large scales. To quantify how fast the turbulence develops in the reconnection jets, we estimate the travel time τ_t of the jet, i.e., the time it takes for a plasma parcel to travel from the X-line to the spacecraft, which is the maximum time for turbulence to develop. Assuming an Alfvénic outflow, we get $\tau_t = \delta x_t/V_{A0}$, where $V_{A0} = B_0/\sqrt{\mu_0 n_i m_i}$ is the Alfvén speed in the background field and δx_t is the jet travel distance between the location of the spacecraft and the statistical location of the reconnection X-line [28,88,89]. We normalize the travel time to $f_{ci0} = eB_0/2\pi m_i$ as $\tau_t f_{ci0} = (2\pi)^{-1} \delta x_t/d_i$. From Fig. 3(b), we

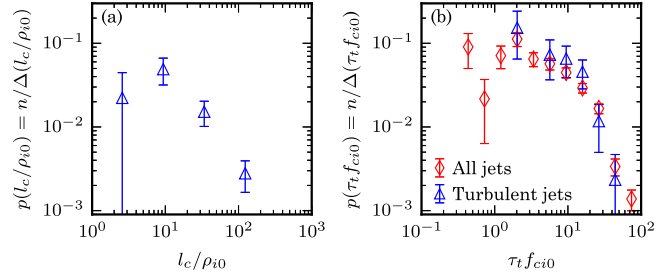


FIG. 3. Histograms of (a) the correlation scales and (b) the travel time of the jets. Blue triangles correspond to the 24 reconnection jets studied here and the red diamonds to the entire dataset.

see that the distribution of 24 reconnection jets where we find statistical signatures of fully developed turbulence mirrors that of the entire dataset of 330 cases. However, none of the 31 jets observed within $\tau_t f_{ci0} \leq 1$ showed signatures of fully developed turbulence. We find that the median travel time of the turbulent jets is $\tau_t f_{ci0} \approx 7.2^{+7.8}_{-3.2}$, so that $\delta x_t/d_i \approx 45^{+49}_{-20}$. Development of turbulent fluctuations at similar distances ($> 30d_i$) from the reconnection X-line has been observed in simulations [90]. Our result suggests that the turbulence can reach a well-developed state already after a few ion gyroperiods.

At scales $l_\perp \ll \rho_i$, we also observe that the scaling exponents $\zeta(m)/\zeta(3)$, with $\zeta(3) = 2.3 \pm 0.2$, show a weakly nonlinear monotonic increase with m [Fig. 2(d)]. In addition, the flatness monotonically increases as the scale decreases [Fig. 2(e)], indicating intermittent energy transfer at sub-ion scales. This contrasts with previous observations in other environments [91–94] and might be due to the growth of kinetic scale instabilities such as the ion and electron tearing modes [12,95] or the electron Kelvin-Helmholtz instability [96]. Using the multifractal p model of energy cascade with $\alpha = 2.85 \pm 0.03$ yields an intermittency parameter $p = 0.568 \pm 0.005$ close to monofractal ($p = 0.5$). This indicates that, in contrast with the large scales, the sub-ion scale fluctuations are predominantly waves rather than turbulence.

At sub-ion scales, kinetic processes can grow into wave modes such as kinetic Alfvén waves (KAWs) or whistler waves. Theoretical analysis of the electron-reduced MHD [50] and Hall MHD [97] suggested that nonlinear interactions among these waves can result in an energy cascade at sub-ion scales. Kinetic-scale waves in the magnetotail plasma jets have been suggested to be KAWs [98]. To investigate the sub-ion scales energy transfer, we estimate the phase speed of the electromagnetic fluctuations in the plasma frame $V_{ph}^{\text{jet}} = |\delta E_\perp|/|\delta B_\perp| - V$ and compare with the prediction for KAWs [48,51,99] with $|\mathbf{k}_\perp| = |\mathbf{k}|$ having verified that $|\mathbf{k}_\perp| \gg k_\parallel$ (see Supplemental Material [40]). The phase speed of the electromagnetic fluctuations shows a clear dispersive

behaviour, $V_{ph}^{\text{jet}}/V_A \propto |\mathbf{k}_\perp|$, in excellent agreement with the prediction for KAWs (see also Supplemental Material [40]).

We have presented a complete systematic statistical description of turbulence in a sample of 24 reconnection jets observed by MMS. We find that the energy is injected at the characteristic scale of the jet and that turbulence transfers energy across a limited inertial range. The average zeroth-order estimate of the energy transfer rate in the MHD framework is $\langle e \rangle = 1.8_{-0.7}^{+1.1} \times 10^8 \text{ J kg}^{-1} \text{ s}^{-1}$, which makes reconnection jets the strongest driver of turbulence observed so far in space plasmas [75]. We showed that at sub-ion scales, in contrast with the large scales, the fluctuations are weakly intermittent, indicating that they are mainly waves rather than structures. These waves are predominantly KAWs that may originate from nonlinear interactions among the large-scale fluctuations or kinetic instabilities and can dissipate the energy into plasma heating through, e.g., stochastic heating and Landau damping [100,101]. As a result of the plasma heating, the gyroradii of the particles increase so that they can interact with the large-scale fluctuations at progressively larger scales [23]. Eventually, the suprathermal particles are accelerated by the large-scale electric field of the jet [102]. Thus, the jet-generated turbulence is a staircase for seed particles to climb in energy. This scenario could explain the observation of supra-thermal ion gamma-ray flares at nebula [103] and active galactic nuclei [104]. Our results also provide new insights into the interplay between turbulence and magnetic reconnection. We show that reconnection outflows drive a strong turbulent cascade, which is an essential part of the fast turbulent MHD reconnection model [1] and can be relevant to the generation of solar wind turbulence [105] by reconnection in the solar corona [106,107].

MMS data are available at the MMS Science Data Center; see Ref. [108]. Data analysis was performed using the PYRFU analysis package [109].

We thank the MMS team and instrument PIs for data access and support. This work was supported by the Swedish National Space Agency (SNSA) Grants 139/18 and 145/18, and by the Swedish Research Council (VR) Research Grant 2022-03352.

- [4] S. Masuda, T. Kosugi, H. Hara, S. Tsuneta, and Y. Ogawara, *Nature (London)* **371**, 495 (1994).
- [5] B. Ripperda, M. Liska, K. Chatterjee, G. Musoke, A. A. Philippov, S. B. Markoff, A. Tchekhovskoy, and Z. Younsi, *Astrophys. J. Lett.* **924**, L32 (2022).
- [6] Y. V. Khotyaintsev, D. B. Graham, C. Norgren, and A. Vaivads, *Front. Astron. Space Sci.* **6**, 70 (2019).
- [7] D. Biskamp, *Magnetohydrodynamic Turbulence* (Cambridge University Press, Cambridge, England, 2003).
- [8] U. Frisch, *Turbulence: The Legacy of A. N. Kolmogorov* (Cambridge University Press, Cambridge, England, 1995).
- [9] H. Karimabadi, V. Roytershteyn, M. Wan, W. H. Matthaeus, W. Daughton, P. Wu, M. Shay, B. Loring, J. Borovsky, E. Leonardis, S. C. Chapman, and T. K. M. Nakamura, *Phys. Plasmas* **20**, 012303 (2013).
- [10] W. H. Matthaeus, *Phys. Plasmas* **28**, 032306 (2021).
- [11] G. Lapenta, S. Markidis, M. V. Goldman, and D. L. Newman, *Nat. Phys.* **11**, 690 (2015).
- [12] E. Leonardis, S. C. Chapman, W. Daughton, V. Roytershteyn, and H. Karimabadi, *Phys. Rev. Lett.* **110**, 205002 (2013).
- [13] F. Pucci, S. Servidio, L. Sorriso-Valvo, V. Olshevsky, W. H. Matthaeus, F. Malara, M. V. Goldman, D. L. Newman, and G. Lapenta, *Astrophys. J.* **841**, 60 (2017).
- [14] Z. Vörös, W. Baumjohann, R. Nakamura, M. Volwerk, and A. Runov, *Space Sci. Rev.* **122**, 301 (2006).
- [15] S. Y. Huang, M. Zhou, F. Sahraoui, A. Vaivads, X. H. Deng, M. André, J. S. He, H. S. Fu, H. M. Li, Z. G. Yuan, and D. D. Wang, *Geophys. Res. Lett.* **39**, L11104 (2012).
- [16] K. T. Osman, K. H. Kiyani, W. H. Matthaeus, B. Hnat, S. C. Chapman, and Y. V. Khotyaintsev, *Astrophys. J.* **815**, L24 (2015).
- [17] R. Jin, M. Zhou, Y. Pang, X. Deng, and Y. Yi, *Astrophys. J.* **925**, 17 (2022).
- [18] H. S. Fu, A. Vaivads, Y. V. Khotyaintsev, M. André, J. B. Cao, V. Olshevsky, J. P. Eastwood, and A. Retinò, *Geophys. Res. Lett.* **44**, 37 (2017).
- [19] J. T. Dahlin, J. F. Drake, and M. Swisdak, *Phys. Plasmas* **24**, 092110 (2017).
- [20] X. Li, F. Guo, H. Li, A. Stanier, and P. Kilian, *Astrophys. J.* **884**, 118 (2019).
- [21] Q. Zhang, F. Guo, W. Daughton, H. Li, and X. Li, *Phys. Rev. Lett.* **127**, 185101 (2021).
- [22] H. Arnold, J. F. Drake, M. Swisdak, F. Guo, J. T. Dahlin, B. Chen, G. Fleishman, L. Glesener, E. Kontar, T. Phan, and C. Shen, *Phys. Rev. Lett.* **126**, 135101 (2021).
- [23] S. Dalena, A. F. Rappazzo, P. Dmitruk, A. Greco, and W. H. Matthaeus, *Astrophys. J.* **783**, 143 (2014).
- [24] V. Zhdankin, D. A. Uzdensky, G. R. Werner, and M. C. Begelman, *Phys. Rev. Lett.* **122**, 055101 (2019).
- [25] M. Lemoine, *Phys. Rev. Lett.* **129**, 215101 (2022).
- [26] T. Dudok De Wit, *Phys. Rev. E* **70**, 055302(R) (2004).
- [27] J. L. Burch, T. E. Moore, R. B. Torbert, and B. L. Giles, *Space Sci. Rev.* **199**, 5 (2016).
- [28] L. Richard, Y. V. Khotyaintsev, D. B. Graham, and C. T. Russell, *Geophys. Res. Lett.* **49**, e2022GL101693 (2022).
- [29] V. Angelopoulos, J. P. McFadden, D. Larson, C. W. Carlson, S. B. Mende, H. Frey, T. Phan, D. G. Sibeck, K.-H. Glassmeier, U. Auster, E. Donovan, I. R. Mann,

*louis.richard@irfu.se

- [1] A. Lazarian, G. Eyink, E. Vishniac, and G. Kowal, *Phil. Trans. R. Soc. A* **373**, 20140144 (2015).
- [2] D. Biskamp, *Magnetic Reconnection in Plasmas*, Cambridge Monographs on Plasma Physics (Cambridge University Press, Cambridge, England, 2000).
- [3] M. Yamada, R. Kulsrud, and H. Ji, *Rev. Mod. Phys.* **82**, 603 (2010).

- I. J. Rae, C. T. Russell, A. Runov, X.-Z. Zhou, and L. Kepko, *Science* **321**, 931 (2008).
- [30] V. Angelopoulos, A. Runov, X.-Z. Zhou, D. L. Turner, S. A. Kiehas, S.-S. Li, and I. Shinohara, *Science* **341**, 1478 (2013).
- [31] P. L. Pritchett and F. V. Coroniti, *J. Geophys. Res.* **115**, A06301 (2010).
- [32] E. V. Panov, R. Nakamura, W. Baumjohann, M. G. Kubyshkina, A. V. Artemyev, V. A. Sergeev, A. A. Petrukovich, V. Angelopoulos, K.-H. Glassmeier, J. P. McFadden, and D. Larson, *J. Geophys. Res.* **117**, 2011JA017496 (2012).
- [33] C. T. Russell, B. J. Anderson, W. Baumjohann, K. R. Bromund, D. Dearborn, D. Fischer, G. Le, H. K. Leinweber, D. Leneman, W. Magnes, J. D. Means, M. B. Moldwin, R. Nakamura, D. Pierce, F. Plaschke, K. M. Rowe, J. A. Slavin, R. J. Strangeway, R. Torbert, C. Hagen, I. Jernej, A. Valavanoglou, and I. Richter, *Space Sci. Rev.* **199**, 189 (2016).
- [34] P.-A. Lindqvist, G. Olsson, R. B. Torbert, B. King, M. Granoff, D. Rau, G. Needell, S. Turco, I. Dors, P. Beckman, J. Macri, C. Frost, J. Salwen, A. Eriksson, L. Åhlén, Y. V. Khotyaintsev, J. Porter, K. Lappalainen, R. E. Ergun, W. Wermeer, and S. Tucker, *Space Sci. Rev.* **199**, 137 (2016).
- [35] R. E. Ergun, S. Tucker, J. Westfall, K. A. Goodrich, D. M. Malaspina, D. Summers, J. Wallace, M. Karlsson, J. Mack, N. Brennan, B. Pyke, P. Withnell, R. Torbert, J. Macri, D. Rau, I. Dors, J. Needell, P.-A. Lindqvist, G. Olsson, and C. M. Cully, *Space Sci. Rev.* **199**, 167 (2016).
- [36] C. Pollock *et al.*, *Space Sci. Rev.* **199**, 331 (2016).
- [37] D. J. Gershman, J. C. Dorelli, L. A. Avanov, U. Gliese, A. Barrie, C. Schiff, D. E. Da Silva, W. R. Paterson, B. L. Giles, and C. J. Pollock, *J. Geophys. Res.* **124**, 10345 (2019).
- [38] W. H. Matthaeus, S. Oughton, D. H. Pontius, and Y. Zhou, *J. Geophys. Res.* **99**, 19267 (1994).
- [39] G. K. Batchelor, *The Theory of Homogeneous Turbulence* (Cambridge University Press, Cambridge, England, 1953).
- [40] See Supplemental Material at <http://link.aps.org/supplemental/10.1103/PhysRevLett.132.105201> for a description of the formulations of the third-order law and the validation of Taylor's hypothesis, wave-vector anisotropy, the ergodicity theorem, and the statistical convergence, which includes Refs. [14,15,26,41–70].
- [41] G. I. Taylor, *Proc. R. Soc. A* **164**, 476 (1938).
- [42] G. G. Howes, K. G. Klein, and J. M. TenBarge, *Astrophys. J.* **789**, 106 (2014).
- [43] H. Politano and A. Pouquet, *Phys. Rev. E* **57**, R21 (1998).
- [44] B. T. MacBride, C. W. Smith, and M. A. Forman, *Astrophys. J.* **679**, 1644 (2008).
- [45] N. Andrés and F. Sahraoui, *Phys. Rev. E* **96**, 053205 (2017).
- [46] N. Andrés, F. Sahraoui, S. Galtier, L. Z. Hadid, R. Ferrand, and S. Y. Huang, *Phys. Rev. Lett.* **123**, 245101 (2019).
- [47] R. Bandyopadhyay, A. Chasapis, D. J. Gershman, B. L. Giles, C. T. Russell, R. J. Strangeway, O. Le Contel, M. R. Argall, and J. L. Burch, *Mon. Not. R. Astron. Soc.* **500**, L6 (2020).
- [48] K. Stasiewicz, P. Bellan, C. Chaston, C. Kletzing, R. Lysak, J. Maggs, O. Pokhotelov, C. Seyler, P. Shukla, L. Stenflo, A. Strelnsov, and J.-E. Wahlund, *Space Sci. Rev.* **92**, 423 (2000).
- [49] C. Meneveau and K. R. Sreenivasan, *Phys. Rev. Lett.* **59**, 1424 (1987).
- [50] A. A. Schekochihin, S. C. Cowley, W. Dorland, G. W. Hammett, G. G. Howes, E. Quataert, and T. Tatsuno, *Astrophys. J. Suppl. Ser.* **182**, 310 (2009).
- [51] S. Boldyrev, K. Horaites, Q. Xia, and J. C. Perez, *Astrophys. J.* **777**, 41 (2013).
- [52] E. N. Parker, *J. Geophys. Res.* **62**, 509 (1957).
- [53] C. C. Haggerty, M. A. Shay, A. Chasapis, T. D. Phan, J. F. Drake, K. Malakit, P. A. Cassak, and R. Kieokaew, *Phys. Plasmas* **25**, 102120 (2018).
- [54] J. E. Stawarz *et al.*, *J. Geophys. Res.* **121**, 11021 (2016).
- [55] D. B. Graham, Y. V. Khotyaintsev, A. Vaivads, and M. André, *J. Geophys. Res.* **121**, 3069 (2016).
- [56] D. B. Graham, Y. V. Khotyaintsev, C. Norgren, A. Vaivads, M. André, J. F. Drake, J. Egedal, M. Zhou, O. Le Contel, J. M. Webster, B. Lavraud, I. Kacem, V. Génot, C. Jacquay, A. C. Rager, D. J. Gershman, J. L. Burch, and R. E. Ergun, *J. Geophys. Res.* **124**, 8727 (2019).
- [57] J. Vogt, S. Haaland, and G. Paschmann, *Ann. Geophys.* **29**, 2239 (2011).
- [58] F. Sahraoui, M. L. Goldstein, G. Belmont, P. Canu, and L. Rezeau, *Phys. Rev. Lett.* **105**, 131101 (2010).
- [59] F. Sahraoui, G. Belmont, L. Rezeau, N. Cornilleau-Wehrlin, J. L. Pinçon, and A. Balogh, *Phys. Rev. Lett.* **96**, 075002 (2006).
- [60] J. L. Pinçon and F. Lefèuvre, *J. Geophys. Res.* **96**, 1789 (1991).
- [61] J. P. Eastwood, T. D. Phan, S. D. Bale, and A. Tjulin, *Phys. Rev. Lett.* **102**, 035001 (2009).
- [62] C. W. Smith, W. H. Matthaeus, G. P. Zank, N. F. Ness, S. Oughton, and J. D. Richardson, *J. Geophys. Res.* **106**, 8253 (2001).
- [63] K. Kiyani, S. C. Chapman, and B. Hnat, *Phys. Rev. E* **74**, 051122 (2006).
- [64] J. E. Stawarz, C. W. Smith, B. J. Vasquez, M. A. Forman, and B. T. MacBride, *Astrophys. J.* **697**, 1119 (2009).
- [65] J. W. Bieber, W. Wanner, and W. H. Matthaeus, *J. Geophys. Res.* **101**, 2511 (1996).
- [66] Y. Wang, R. Chhiber, S. Adhikari, Y. Yang, R. Bandyopadhyay, M. A. Shay, S. Oughton, W. H. Matthaeus, and M. E. Cuesta, *Astrophys. J.* **937**, 76 (2022).
- [67] P. Simon and F. Sahraoui, *Phys. Rev. E* **105**, 055111 (2022).
- [68] S. P. Gary and C. W. Smith, *J. Geophys. Res.* **114**, A12105 (2009).
- [69] C. H. K. Chen, S. Boldyrev, Q. Xia, and J. C. Perez, *Phys. Rev. Lett.* **110**, 225002 (2013).
- [70] D. Grošelj, A. Mallet, N. F. Loureiro, and F. Jenko, *Phys. Rev. Lett.* **120**, 105101 (2018).
- [71] A. Kolmogorov, *Akademii Nauk SSSR Doklady* **30**, 301 (1941).
- [72] L. Matteini, O. Alexandrova, C. H. K. Chen, and C. Lacombe, *Mon. Not. R. Astron. Soc.* **466**, 945 (2017).
- [73] J. E. Stawarz, L. Matteini, T. N. Parashar, L. Franci, J. P. Eastwood, C. A. Gonzalez, I. L. Gingell, J. L. Burch, R. E. Ergun, N. Ahmadi, B. L. Giles, D. J. Gershman, O. Le Contel, P.-A. Lindqvist, C. T. Russell, R. J. Strangeway,

- and R. B. Torbert, *J. Geophys. Res.* **126**, 2020JA028447 (2021).
- [74] G. Paladin and A. Vulpiani, *Phys. Rep.* **156**, 147 (1987).
- [75] R. Marino and L. Sorriso-Valvo, *Phys. Rep.* **1006**, 1 (2023).
- [76] K. T. Osman, M. Wan, W. H. Matthaeus, J. M. Weygand, and S. Dasso, *Phys. Rev. Lett.* **107**, 165001 (2011).
- [77] L. Z. Hadid, F. Sahraoui, S. Galtier, and S. Y. Huang, *Phys. Rev. Lett.* **120**, 055102 (2018).
- [78] L. Sorriso-Valvo *et al.*, *Phys. Rev. Lett.* **122**, 035102 (2019).
- [79] A. V. Artemyev, A. A. Petrukovich, R. Nakamura, and L. M. Zelenyi, *J. Geophys. Res.* **115**, A12255 (2010).
- [80] Y. Asano, T. Mukai, M. Hoshino, Y. Saito, H. Hayakawa, and T. Nagai, *J. Geophys. Res.* **108**, 1189 (2003).
- [81] R. Nakamura, W. Baumjohann, C. Mouikis, L. M. Kistler, A. Runov, M. Volwerk, Y. Asano, Z. Vörös, T. L. Zhang, B. Klecker, H. Rème, and A. Balogh, *Geophys. Res. Lett.* **31**, L09804 (2004).
- [82] J. Liu, V. Angelopoulos, A. Runov, and X.-Z. Zhou, *J. Geophys. Res.* **118**, 2000 (2013).
- [83] M. Wan, S. Oughton, S. Servidio, and W. H. Matthaeus, *J. Fluid Mech.* **697**, 296 (2012).
- [84] M. F. Linkmann, A. Berera, W. D. McComb, and M. E. McKay, *Phys. Rev. Lett.* **114**, 235001 (2015).
- [85] E. R. Priest and T. Forbes, *Magnetic Reconnection: MHD Theory and Applications* (Cambridge University Press, Cambridge, England, 2000).
- [86] A. S. Sharma, R. Nakamura, A. Runov, E. E. Grigorenko, H. Hasegawa, M. Hoshino, P. Louarn, C. J. Owen, A. Petrukovich, J.-A. Sauvaud, V. S. Semenov, V. A. Sergeev, J. A. Slavin, B. U. Ö. Sonnerup, L. M. Zelenyi, G. Fruit, S. Haaland, H. Malova, and K. Snekvik, *Ann. Geophys.* **26**, 955 (2008).
- [87] R. Benzi, S. Ciliberto, R. Tripiccione, C. Baudet, F. Massaioli, and S. Succi, *Phys. Rev. E* **48**, R29 (1993).
- [88] L. Richard, Y. V. Khotyaintsev, D. B. Graham, A. Vaivads, D. J. Gershman, and C. T. Russell, *Phys. Rev. Lett.* **131**, 115201 (2023).
- [89] T. Nagai, M. Fujimoto, R. Nakamura, W. Baumjohann, A. Ieda, I. Shinohara, S. Machida, Y. Saito, and T. Mukai, *J. Geophys. Res.* **110**, A09208 (2005).
- [90] K. Higashimori and M. Hoshino, *J. Geophys. Res.* **120**, 1803 (2015).
- [91] P. Wu, S. Perri, K. Osman, M. Wan, W. H. Matthaeus, M. A. Shay, M. L. Goldstein, H. Karimabadi, and S. Chapman, *Astrophys. J.* **763**, L30 (2013).
- [92] C. H. K. Chen, L. Sorriso-Valvo, J. Šafránková, and Z. Němeček, *Astrophys. J.* **789**, L8 (2014).
- [93] S. S. Cerri, D. Grošelj, and L. Franci, *Front. Astron. Space Sci.* **6**, 64 (2019).
- [94] A. Chasapis, W. H. Matthaeus, R. Bandyopadhyay, R. Chhiber, N. Ahmadi, R. E. Ergun, C. T. Russell, R. J. Strangeway, B. L. Giles, D. J. Gershman, C. J. Pollock, and J. L. Burch, *Astrophys. J.* **903**, 127 (2020).
- [95] A. A. Galeev and L. M. Zelenyi, *Sov. J. Exp. Theor. Phys.* **43**, 1113 (1976).
- [96] H. Che, G. P. Zank, and A. O. Benz, *Astrophys. J.* **921**, 135 (2021).
- [97] S. Galtier, *J. Plasma Phys.* **72**, 721 (2006).
- [98] C. C. Chaston, J. W. Bonnell, L. Clausen, and V. Angelopoulos, *J. Geophys. Res.* **117**, A12205 (2012).
- [99] G. G. Howes, S. C. Cowley, W. Dorland, G. W. Hammett, E. Quataert, and A. A. Schekochihin, *Astrophys. J.* **651**, 590 (2006).
- [100] D. J. Gershman, A. F-Viñas, J. C. Dorelli, S. A. Boardsen, L. A. Avanov, P. M. Bellan, S. J. Schwartz, B. Lavraud, V. N. Coffey, M. O. Chandler, Y. Saito, W. R. Paterson, S. A. Fuselier, R. E. Ergun, R. J. Strangeway, C. T. Russell, B. L. Giles, C. J. Pollock, R. B. Torbert, and J. L. Burch, *Nat. Commun.* **8**, 14719 (2017).
- [101] J. Liang, Y. Lin, J. R. Johnson, Z.-X. Wang, and X. Wang, *Phys. Plasmas* **24**, 102110 (2017).
- [102] L. Richard, Y. V. Khotyaintsev, D. B. Graham, A. Vaivads, R. Nikoukar, I. J. Cohen, D. L. Turner, S. A. Fuselier, and C. T. Russell, *J. Geophys. Res.* **127**, e2022JA030430 (2022).
- [103] M. Tavani *et al.*, *Science* **331**, 736 (2011).
- [104] A. Shukla and K. Mannheim, *Nat. Commun.* **11**, 4176 (2020).
- [105] L.-L. Zhao, G. P. Zank, D. Telloni, M. Stevens, J. C. Kasper, and S. D. Bale, *Astrophys. J. Lett.* **928**, L15 (2022).
- [106] J. F. Drake, O. Agapitov, M. Swisdak, S. T. Badman, S. D. Bale, T. S. Horbury, J. C. Kasper, R. J. MacDowall, F. S. Mozer, T. D. Phan, M. Pulupa, A. Szabo, and M. Velli, *Astron. Astrophys.* **650**, A2 (2021).
- [107] N. E. Raouafi, G. Stenborg, D. B. Seaton, H. Wang, J. Wang, C. E. DeForest, S. D. Bale, J. F. Drake, V. M. Uritsky, J. T. Karpen, C. R. DeVore, A. C. Sterling, T. S. Horbury, L. K. Harra, S. Bourouaine, J. C. Kasper, P. Kumar, T. D. Phan, and M. Velli, *Astrophys. J.* **945**, 28 (2023).
- [108] See <https://lasp.colorado.edu/mmssdc/public>.
- [109] L. Richard, Y. V. Khotyaintsev, A. Vaivads, D. B. Graham, C. Norgren, and A. Johlander, Zenodo (2024), [10.5281/zenodo.10678695](https://doi.org/10.5281/zenodo.10678695).